

## A Monte-Carlo Study of the Role of Scattering in Deca-nanometer MOSFETs

P. Palestri, D. Esseni, S. Eminentè†, C. Fiegna\*†, E. Sangiorgi†† and L. Selmi

DIEG, Univ. of Udine, Via delle Scienze 208, 33100 Udine, Italy, FAX: +39-0432-558251, e.mail: palestri@uniud.it

† ARCES Center, Bologna, Italy

\* ENDIF, Univ. of Ferrara, Italy

+ DEIS, Univ. of Bologna, Italy

### AREA: MODELING AND SIMULATION

The ITRS roadmap [1] projects the introduction of MOSFETs with gate length  $L_G \leq 25nm$  by the year 2007. The accurate modeling of these devices is a challenging objective, since both quantization and non-equilibrium transport effects have to be properly taken into account. A tempting simplification consists in neglecting the scattering and develop ballistic transport models [2]. However, the *a-priori* assumption of the negligible role of scattering is difficult to justify.

*In this paper, a Monte-Carlo simulator including quantum corrections to the potential is used to study electronic transport in double gate (DG) SOI MOSFETs with  $L_G$  down to 14nm. Our results demonstrate that, for the explored  $L_G$  values, scattering still controls the ON current ( $I_{DS}$ ), which for  $L_G = 25nm$  is overestimated by about a factor of 2 in the ballistic model. By monitoring the electrons back-scattered at the source, we discuss the role of scattering in different parts of the device.*

**Simulation model.** A Full-Band self-consistent Monte Carlo (MC) simulator for the free-electron gas has been adapted to the study of nano-scale MOSFETs. The effect of carrier quantization on the inversion charge ( $N_{INV}$ ) is taken into account by using the effective potential approach [3], that reproduces the  $N_{INV}$  versus  $V_{GS}$  curves of a variety of deeply scaled MOSFETs [4]. The scattering model includes phonons, ionized impurities, carrier-plasmon and surface roughness (SR). Since the effective potential repels the carriers from the interface, the usual specular-diffusive approach to model SR scattering cannot be used. Therefore, SR has been implemented as an additional scattering mechanism [5], whose rate is related to the vertical effective field. Since the MC simulator does not account for sub-band splitting, the reported mobility and scattering rate modulation with the silicon thickness ( $t_{SI}$ ) for  $t_{SI} \leq 10nm$  [6] is not reproduced; furthermore, the simulated injection velocity at the source can slightly differ from that of the 2D electron gas. Since our model reproduces the universal mobility curves (Fig. 1) and we will restrict the analysis to  $t_{SI} \geq 10nm$ , considering ratios between currents, the model is adequate for the problem at hand.

**Scattering in the channel.** Fig. 2 shows the output characteristic ( $I_{DS}$  vs  $V_{DS}$ ) of a 25nm DG SOI MOSFET. The ballistic current  $I_{DS}^{BAL}$  is obtained by turning off scattering inside the channel and inside a portion of the drain much larger than the mean free path, but keeping the scattering active near the source and drain contacts. The important role of scattering even in this ultra-short device is demonstrated by the reduction of the current by about a factor of 2.

To investigate this behavior, Fig. 3 reports the currents due to particles moving from source to drain ( $I^+$ ) and from drain to source ( $I^-$ ). While  $I_{DS} = I^+ - I^-$  is obviously independent of  $x$ ,  $I^+$  and  $I^-$  are not constant along the channel and their largest values occur inside the source and drain, due to the electrons with energy lower than the potential barrier that are moving back and forth. According to [7] the drain current can be understood in terms of the current injected into the channel  $I_{inj}^+ = I^+(x_{inj})$  and the current back-scattered to the source  $I_{inj}^- = I^-(x_{inj})$ , where  $x_{inj}$  is the position of maximum potential energy (inset in Fig. 3). Fig. 4 (dashed line) plots the total number of scattering events per unit length ( $1/\lambda^+$ ) along  $x$ . In the channel  $1/\lambda^+ \approx 0.1nm^{-1}$ , meaning that, for this device and this bias point, one scattering event every 10nm takes place in the channel. Fig. 4 (solid line) also reports the contribution to  $I_{inj}^-$  given by scattering events in different positions. This contribution (obviously 0 for  $x < x_{inj}$ ) is sharply peaked at  $x_{inj}$  and it decays exponentially for  $x > x_{inj}$  (with decay length  $l_{SCATT}$ ), pointing out that the dominant contribution to  $I_{inj}^-$  is given by scattering events close to the potential barrier in agreement with Ref. [7]. Fig. 5 shows that  $l_{SCATT}$  is close to the KT length, i.e. to the distance on which drops a voltage  $KT/q$  [8].

In order to understand the origin of the large discrepancy between  $I_{DS}$  and  $I_{DS}^{BAL}$  shown in Fig. 2, we relate  $[I_{DS}/I_{DS}^{BAL}]$  to the reflection coefficient  $r = [I_{inj}^-/I_{inj}^+]$  (see Fig. 6). We see that  $[I_{DS}/I_{DS}^{BAL}]$  is lower than  $1 - r = [I_{DS}/I_{inj}^+]$ , because, as demonstrated in Fig. 7, when scattering is turned off, besides having  $I_{inj}^- = 0$ ,  $I_{inj}^+$  increases. Note that if  $N_{INV}(x_{inj})$  is the same with and without scattering, and if the velocities ( $v_{inj}^+$  and  $v_{inj}^-$ ) of carriers belonging to the  $I^+$  and  $I^-$  fluxes are equal, then  $[I_{DS}/I_{DS}^{BAL}] \approx (1 - r)/(1 + r)$  [7]. The latter term (open circles in Fig. 6) is clearly a better description of  $[I_{DS}/I_{DS}^{BAL}]$  than  $1 - r$ . The match, however, is not perfect, mainly because  $x_{inj}$  and  $N_{INV}(x_{inj})$  are not exactly the same in the two cases with and without scattering. This is due to the back-scattered electrons that increase the inversion charge (Fig. 8), so that the potential profile changes (Fig. 9). Furthermore,  $v_{inj}^+$  and  $v_{inj}^-$  are also somewhat different.

**Scattering inside the drain.** It has been suggested that in ultra-short devices back-scattering at the drain could have a relevant impact on  $I_{DS}$  [9, 10]. We have seen in Fig. 4 that the contribution to  $I_{inj}^-$  due to scattering at the drain is negligible, and Fig. 10 (filled squares) confirms that this is the case also in a shorter device. If the scattering inside the channel is turned off (as done in [9, 10]) the contribution to  $I_{inj}^-$  due to back-scattering at the drain becomes much higher (filled circles), and even larger if plasmon scattering in the drain is switched off (open circles). This is because particles injected in a ballistic channel enter the drain with an energy higher than the source barrier. Therefore, if back-scattered by elastic collisions, they travel all the way back to the source, thus contributing to  $I_{inj}^-$ . Plasmons reduce the back-scattered flux, because they efficiently thermalize the hot electrons entering the drain. On the other hand, if inelastic scattering in the channel (e.g. optical phonons) reduces the carrier energy, then carriers entering the drain do not have enough energy to be back-scattered to the source barrier.

**Conclusion.** *Accurate Monte-Carlo simulations demonstrate that scattering still controls the ON current of decanometer devices. The main role is played by scattering events near the source barrier. The effect of scattering on  $I_{DS}$  is not simply proportional to the number of back-scattering events, since self-consistency changes the potential profile, and consequently, the electron flux injected at the source. Due to the inelastic scattering inside the channel, back-scattering at the drain is negligible.*

- [1] *International Technology Roadmap for Semiconductor, 2003.*
- [2] D. Munteanu et al., *Solid State Electronics*, vol. 47, p. 1219, 2003.
- [3] D. K. Ferry et al., *IEDM Technical Digest*, p. 287, 2000.
- [4] P. Palestri et al., *Proc. European Solid State Device Res. Conf.*, p. 407, 2003.
- [5] P. Palestri et al., *Proc. Workshop ULIS*, p. 101, 2004, *submitted to Solid State Elec.*
- [6] D. Esseni et al., *IEEE T-ED*, vol. 48, p. 2842, 2001.
- [7] M. Lundstrom et al., *IEEE T-ED*, vol. 49, p. 133, 2002.
- [8] M. Lundstrom, *IEEE EDL*, vol. 18, p. 361, 1997.
- [9] A. Svizhenko et al., *IEEE T-ED*, vol. 50, p. 1459, 2003.
- [10] M. Mouis et al., *Proc. European Solid State Device Res. Conf.*, p. 147, 2003.
- [11] S. Takagi et al., *IEEE T-ED*, vol. 41, p. 2357, 1994.
- [12] J. Koga et al., *IEEE T-ED*, vol. 49, p. 1043, 2002.

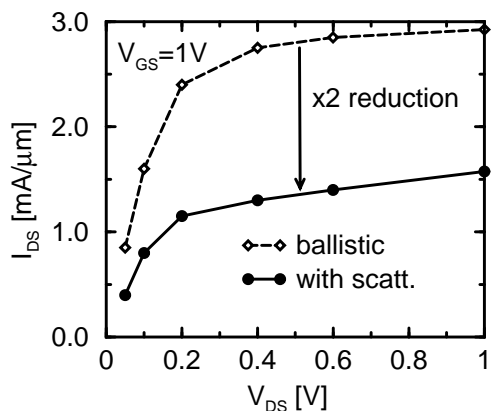


Figure 2: Output characteristics of a double-gate SOI transistor. Solid line: scattering activated in the whole device. Dashed line: ballistic simulation (see text).

Scattering reduces the drain current by about a factor of 2.  $L_G = 25nm$ ,  $t_{SI} = 10nm$ ,  $t_{FOX} = t_{BOX} = 1.26nm$ . The relative dielectric constant is  $\epsilon_{eff} = 7$ .

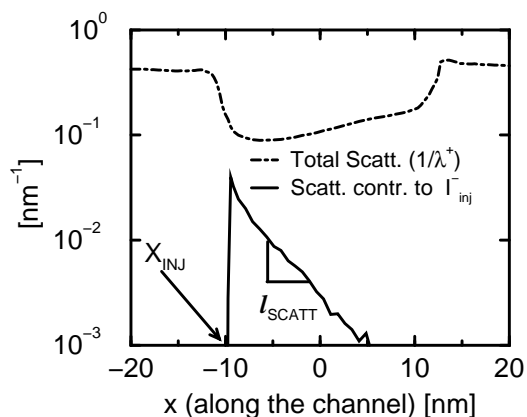


Figure 4: Dashed line: number of scattering events, per unit length, suffered by the electrons moving from source to drain (group velocity  $v_{gx} > 0$ ):

$1/\lambda^+ = q \left( \int_{v_{gx} > 0} f(\vec{k}) \tau^{-1}(\vec{k}) d\vec{k} \right) / I_{inj}^+$ , where  $\tau^{-1}(\vec{k})$  is the total scattering rate (all mechanisms) and  $f(\vec{k})$  is the carrier distribution. Solid line: number of scattering events contributing to  $I_{inj}^-$ , per unit length and unit time, normalized to  $I_{inj}^+ / q$ . This is evaluated by counting the number of particles crossing the section  $x_{inj}$ , with group velocity  $v_{gx} < 0$ , that were back-scattered by a scattering event in a spatial interval  $\Delta x$  placed around the position  $x$ . This number is then divided by  $\Delta x$ , by the simulation time, and by  $I_{inj}^+ / q$ . Same device as in Fig. 2.  $V_{GS} = V_{DS} = 1V$ .

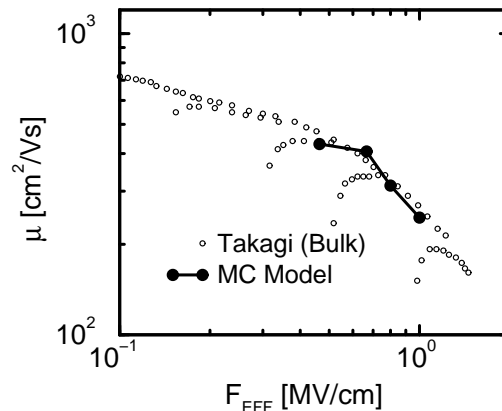


Figure 1: Comparison between the mobility model of our MC simulator (considering only phonon and surface roughness scattering) and the universal mobility curves for bulk devices [11]. As documented in [6, 12], the mobility of SOI MOSFETs with  $t_{Si} \geq 10nm$  is an unique function of the effective field and agrees very well with the universal curves for bulk MOSFETs shown here.

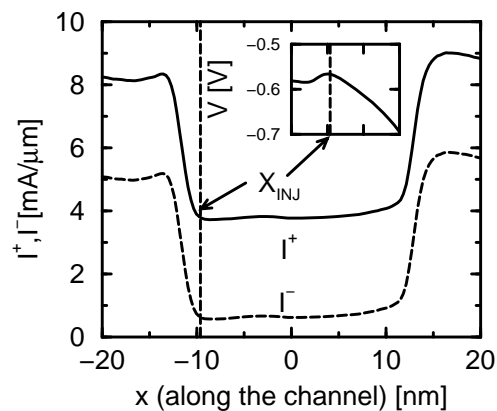


Figure 3: Electron currents due to particles moving from source to drain ( $I^+$ ) and from drain to source ( $I^-$ ) as a function of the position  $x$  along the channel. Same device as in Fig. 2.  $V_{GS} = V_{DS} = 1V$ . The inset plots the average effective potential energy profile close to the source barrier.

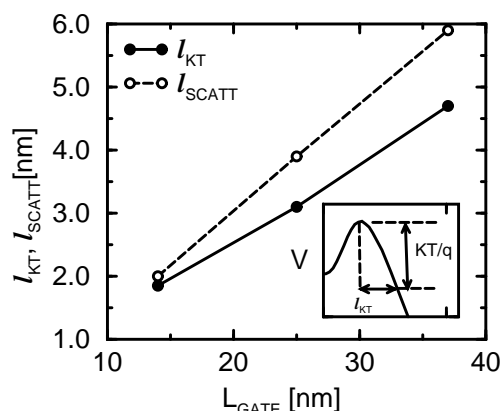


Figure 5: Comparison between the decay length  $l_{SCATT}$  (see solid line in Fig. 4) and the KT length  $l_{KT}$  (i.e. the distance on which drops  $KT/q$ , see the inset).

We note that these two lengths have very similar values (within 20%) and that are both proportional to  $L_G$ .

The devices are similar to the one in Fig. 2, except for the channel length.  $V_{GS} = V_{DS} = 1V$ .

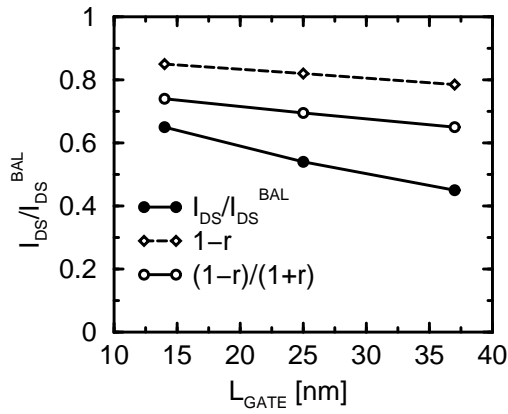


Figure 6: Filled symbols: ratio between the drain current obtained with the scattering activated in the whole device ( $I_{DS}$ ) and with the ballistic simulation ( $I_{DS}^{BAL}$ , scattering turned off inside the channel and in the first part of the drain). Open symbols: terms  $1-r$  (diamonds) and  $(1-r)/(1+r)$  (circles).  $r = I_{inj}^- / I_{inj}^+$ . All these terms increase for reduced  $L_G$ . Same devices as in Fig. 5.  $V_{GS} = V_{DS} = 1V$ .

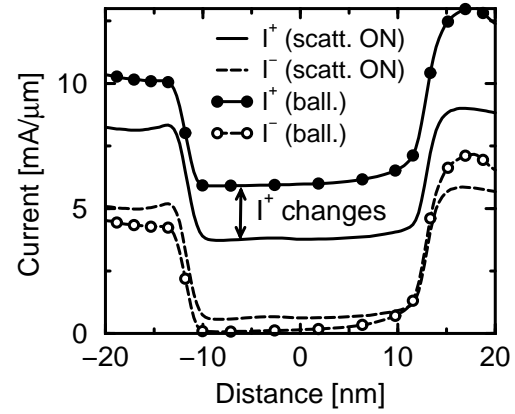


Figure 7:  $I^+$  (solid lines) and  $I^-$  (dashed lines) profiles comparing the case with and without scattering. When scattering is turned off,  $I_{inj}^-$  becomes practically 0, and  $I_{inj}^+$  increases. Same device as in Fig. 2.  $V_{GS} = V_{DS} = 1V$ .

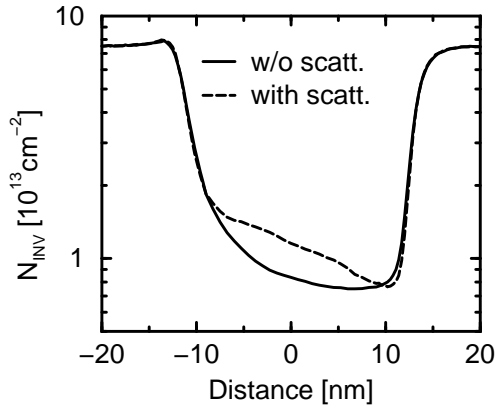


Figure 8: Inversion charge profile along the device. The case without scattering (solid line) is compared with the case with scattering (dashed line). Note the increase of the inversion charge in the channel when scattering is turned on. Same device as in Fig. 2.  $V_{GS} = V_{DS} = 1V$ .

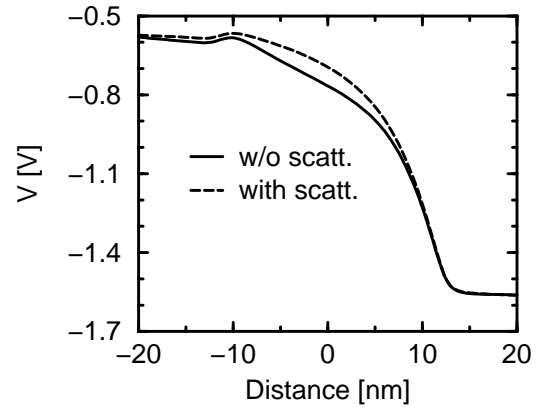


Figure 9: Potential energy profile along the device. The case without scattering (solid line) is compared with the case with scattering (dashed line). Since  $N_{INV}$  is different in the two cases (Fig. 8), the potential profiles differ. Same device as in Fig. 2.  $V_{GS} = V_{DS} = 1V$ .

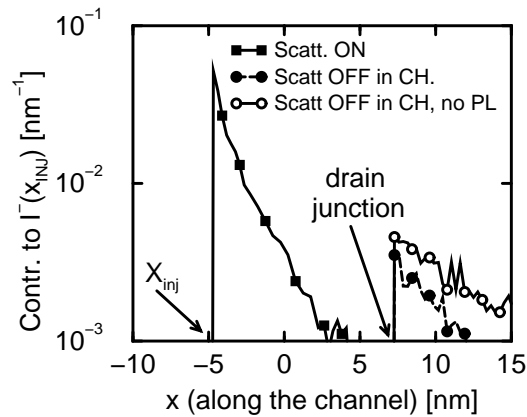


Figure 10: Contribution to  $I_{inj}^-$  given by the scattering at a given position. Filled squares: the scattering is activated in the whole device as in Fig. 4. Filled circles: all scatterings are turned off inside the channel. Open circles: all scatterings are turned off inside the channel (as in [9, 10]), plasmon scattering is turned off also inside the drain. We see back-scattering from the drain only when scattering is turned off inside the channel. Drain back-scattering is higher if plasmon scattering in the drain is not active. The device is similar to that in Fig. 2, except that  $L_G = 14nm$ .  $V_{GS} = V_{DS} = 1V$ .

## **A Monte-Carlo Study of the Role of Scattering in Deca-nanometer MOSFETs**

P. Palestri, D. Esseni, S. Eminentè<sup>†</sup>, C. Fiegna\*<sup>†</sup>, E. Sangiorgi<sup>†+</sup> and L. Selmi

DIEG, Univ. of Udine, Via delle Scienze 208, 33100 Udine, Italy, FAX: +39-0432-558251, e.mail: palestri@uniud.it

<sup>†</sup> ARCES Center, Bologna, Italy      \* ENDIF, Univ. of Ferrara, Italy      + DEIS, Univ. of Bologna, Italy

**AREA: MODELING AND SIMULATION**

### **50 WORDS ABSTRACT**

Monte-Carlo simulations of double-gate SOI MOSFETs with  $L_g$  down to 14nm are reported, showing that scattering in the channel still controls the ON current. For  $L_g=25\text{nm}$ , this is overestimated by about a factor of 2 by ballistic models. The importance of scattering in different parts of the device is discussed.